Entanglement entropy with localized and extended interface defects

Ferenc Iglói
Research Institute for Solid State Physics and Optics, H-1525 Budapest, P.O.Box 49, Hungary and Institute of Theoretical Physics, Szeged University, H-6720 Szeged, Hungary

Zsolt Szatmári
Institute of Theoretical Physics, Szeged University, H-6720 Szeged, Hungary

Yu-Cheng Lin
Theoretische Physik, Universität des Saarlandes, D-66041 Saarbrücken, Germany

(Dated: March 23, 2009)

The quantum Ising chain of length, L, which is separated into two parts by localized or extended defects is considered at the critical point where scaling of the interface magnetization is non-universal. We measure the entanglement entropy between the two halves of the system in equilibrium, as well as after a quench, when the interaction at the interface is changed for time $t > 0$. For the localized defect the increase of the entropy with $\log L$ or with $\log t$ involves the same effective central charge, which is a continuous function of the strength of the defect. On the contrary for the extended defect the equilibrium entropy is saturated, but the non-equilibrium entropy has a logarithmic time-dependence the prefactor of which depends on the strength of the defect.

I. INTRODUCTION

Entanglement, quantum nonlocality and quantum correlations has became the subject of intensive research recently in different fields of physics[1]: quantum information theory, condensed matter physics, quantum field theory, etc. For a quantum system which is divided into two parts, $\mathcal{A}$ and $\mathcal{B}$, all information about entanglement is encoded in the reduced density matrix: $\rho_{\mathcal{A}} = Tr_{\mathcal{B}}|\Psi\rangle\langle\Psi|$, where $|\Psi\rangle$ is a pure state of the complete system. The entanglement between $\mathcal{A}$ and $\mathcal{B}$ is conveniently measured by the von Neumann entropy $S_A = -\mathrm{Tr}_A(\rho_{\mathcal{A}} \log \rho_{\mathcal{A}})$, which has been intensively studied in many-body systems, in particular in one dimension (1d). For a critical 1d system (with periodic boundary conditions) the entropy is found to grow logarithmically with the length, L:

$$S_A = \frac{c}{3} \log L + c_1 \ , \tag{1}$$

where L is the size of $\mathcal{A}$ or the size of the complete system, provided it is divided into two equal parts[2,3,4]. For conformally invariant systems the parameter in the prefactor, c, is universal and given by the central charge of the conformal algebra. In the vicinity of the critical point where the correlation length is $\xi \ll L$, the entropy is saturated and given by:

$$S_A \simeq \frac{c}{3} \log \xi \ . \tag{2}$$

One is also interested in the time evolution of the entropy[5] after changing the form of the interaction (quantum quench) at time $t = 0$. In the case of a local quench[6] the interaction parameters are modified in a restricted region. For example measuring the entropy between $\mathcal{A}$ and $\mathcal{B}$ which are disconnected for $t < 0$ but are joined to a closed chain with homogeneous couplings for $t > 0$ at the critical point we observe a logarithmic increase in time, $t \ll L$, as[7,8]

$$S_A = 2\frac{c}{3} \log t + \mathrm{cst.} \ . \tag{3}$$

If the complete system is open, i.e. there is one boundary point between $\mathcal{A}$ and $\mathcal{B}$ the prefactors in Eqs.(1-3) are divided by a factor 2.

Inhomogeneous interactions could modify the entanglement properties of quantum spin chains. It has been shown that for random[9,10,11,12,13,14,15,16] and aperiodic[17] couplings the prefactor in Eq.(1) is changed and involves the so called effective central charge, c_{eff}. On the other hand if the couplings vary linearly with the position an interface with a certain width is introduced, and in the expression of the entropy in Eq.(2) ξ is replaced by this length[18].

If the inhomogeneities are centered at a few points ("defects") they are not expected to modify the scaling form of the entropy, unless the defects are located at the interface. Indeed interface defects can modify the scaling form of the wavefunction in the vicinity of the junction[19], which in turn alter the entanglement entropy. The effect of a local interface defect, Δ, which measures the coupling between $\mathcal{A}$ and $\mathcal{B}$ has been investigated for XXZ and XX quantum spin chains[20,21,22]. For the antiferromagnetic XXZ chain the defect is a (marginally) relevant perturbation[23], the defect renormalizes to a cut and the effective central charge approaches zero[20]. On the contrary for the ferromagnetic XXZ chain the defect is a (marginally) irrelevant perturbation, the defect renormalizes to the homogeneous coupling and the effective central charge approaches one. Finally, in the XX chain the defect is a marginal perturbation and the effective central charge in Eq.(1) is found[21] to depend on the strength of the defect, Δ.

In the present paper we study the effect of interface de-

fects on the entanglement properties of critical quantum spin chains. Our approach differs from the previous ones in several respects. The system we consider is the quantum Ising chain and we study the problem with a localized as well as with an extended defect. The latter is realized by a smooth inhomogeneity in the couplings varying as $\simeq A/x$, x being the distance from the interface[24,25]. Both perturbations are known to be marginal as far as the scaling behavior of the interface magnetization at the critical point is considered. We study the entropy both in equilibrium, as well as after a quench, when the interface couplings are modified for $t > 0$. The main goal of our investigations is to study possible relations i) between local critical scaling and the scaling of the entropy, and ii) between scaling form of equilibrium and non-equilibrium entropies like in Eqs. (1) and (3).

The structure of the paper is the following. The model, the type of defects, the interface critical behavior as well as the way of calculation of the entropy is described in Sec.II. The localized and the extended defect problems are studied in Sec.III and IV, respectively. Our results are discussed in the final Section. Some technical details of the calculations are put in Appendices.

II. MODELS AND METHOD

We consider the quantum Ising chain defined by the Hamiltonian:

$$H_0 = -\sum_{i=1}^{L} \sigma_i^x \sigma_{i+1}^x - h \sum_{i=1}^{L} \sigma_i^z \tag{4}$$

in terms of the Pauli-matrices, $\sigma_i^{x,z}$, at site i and with periodic boundary conditions, $\sigma_{L+1}^x = \sigma_1^x$. The quantum critical point of the system is given by[26] $h = h_c = 1$, where the bulk correlation function has a power-law decay for large L:

$$G(L) = \langle 0|\sigma_{L/4}^x \sigma_{3L/4}^x|0\rangle \ \sim L^{-\eta} \ , \tag{5}$$

with $\eta = \eta_0 = 1/4$.

A. Localized defect

A localized defect is defined by the perturbation:

$$V_{loc} = (1-\Delta)(\sigma_{L/2}^x \sigma_{L/2+1}^x + \sigma_L^x \sigma_{L+1}^x) \tag{6}$$

so that the complete Hamiltonian is given by $H_0 + V_{loc}$. This perturbation does not modify the decay of the bulk correlations in Eq.(5), however the interface or defect correlations:

$$G_d(L) = \langle 0|\sigma_1^x \sigma_{L/2}^x|0\rangle \ \sim L^{-\eta_d} \ , \tag{7}$$

involve a new exponent[27,28]:

$$\eta_d = \eta_{loc}(\Delta) = \frac{4}{\pi^2} \arctan^2(1/\Delta) \tag{8}$$

which is a continuous function of the strength of the defect, Δ. Note that in the special cases, $\Delta = 0$ and $\Delta = 1$ we recover the known results for surface and bulk correlations, respectively.

More generally, one can consider the defect at position L of different strength, say Δ'. For $\Delta' = 1$ and for $\Delta' = 0$ there is one defect in the closed or open chain, respectively. The defect exponent is then modified to $(\eta_d + 1/4)/2$ and $(\eta_d + 1)/2$, respectively[19].

B. Extended defect

The extended defect is defined by a smooth inhomogeneity[25]:

$$V_{ext} = -\sum_{i=1}^{L} \lambda_i \sigma_i^x \sigma_{i+1}^x, \quad \lambda_i = \frac{A/2}{\frac{L}{2\pi}\left|\sin\left[\frac{2\pi(i-\delta)}{L}\right]\right|} \tag{9}$$

and this perturbation is put symmetrically in the two parts of the lattice. In Eq.(9) we have used a shift, $\delta = O(1)$, in order to avoid singularities.

The local critical behavior of this system is different for $A < 0$ and for $A > 0$. For weakened local couplings, $A < 0$, correlations between two defect spins, $G_d(L)$, has an algebraic decay with an A dependent defect exponent: $\eta_{ext}(A) = 1 - A$. At the same time correlations between two bulk spins, $G(L)$, involves an exponent η which also depends on A: $\eta = 1/4 - A$. This unexpected variation of the exponent with A is due to the fact that the interface coupling at $i = 0$ (as well as at $i = L/2$) renormalizes to zero as $J_0(L) \sim L^A$. This fact explains also the observation that the decay exponent of the end-to-end correlations for two decoupled chains is just $\eta_{ext}(A)$, at least for $A < 0$.

For enhanced local couplings, $A > 0$, the defect-defect correlations, $G_d(L)$, approach a finite limiting value, m_d^2, so that the interface stays ordered at the bulk critical point. The connected correlation function, $G_d(L) - m_d^2$, decays to zero algebraically with an exponent $\eta'_{ext}(A) = 2A$. In this case correlations between bulk spins, $G(L)$, involves the pure exponent, $\eta_0 = 1/4$.

C. Calculation of the entropy

Calculation of the entropy of the quantum Ising chain in the equilibrium case is described in detail in several papers[3,16,30]. The nonequilibrium entropy in the homogeneous case and in the thermodynamic limit is calculated in[5], whereas for inhomogeneous couplings the method is described in the Appendix A. Here we briefly recapitulate the main steps of the calculation and describe the technical steps needed in the numerical calculation.

The first step is to transform the Hamiltonian of the quantum Ising chain in terms of free fermions[29]. Numerically, this step necessitates the diagonalization of an $L \times L$

symmetric matrix. In the second step we calculate the reduced density matrix, which can be reconstructed from the correlation matrix in the free fermionic basis[30]. The entanglement entropy is calculated then from the eigenvalues of the reduced correlation matrix., If $\mathcal{A}$ has ℓ sites (in our case we use $\ell = L/2$) this second step requires the diagonalization of a $\ell \times \ell$ symmetric matrix, if one works with Dirac fermions[16] or a $2\ell \times 2\ell$ skew-symmetric matrix if the calculation is performed with Majorana fermions[3]. At this step we have calculated the so called single-copy entanglement[31], too, which is defined through the largest eigenvalue of the density matrix, w_1, as $S_1 = -\log w_1$. S_1 is obtained also from the eigenvalues of the correlation matrix. For homogeneous chains $S_1(L)$ is known to have a logarithmic size-dependence:

$$S_1 = \frac{\kappa}{3} \log L + \text{cst} \ , \tag{10}$$

with a prefactor: $\kappa = c/2$.

In the third step of the calculation we consider the time evolution of the entropy after a quench. For this we should calculate the time evolution of the correlation matrix[32], which can be done in the Majorana fermion basis. Each matrix-elements is obtained through L^2 operations, which will result in the increase of the computational time accordingly.

If the entropy has a logarithmic dependence, either as a function of the size (see Eq.(1)) or the time (see Eq.(3)), then we have calculated the prefactors through two-point fit and in this way effective central charges are obtained as:

$$c_{eff}(L) = 3[\mathcal{S}(2L) - \mathcal{S}(L)]/\log 2 \ . \tag{11}$$

Similarly in the nonequilibrium case we calculated the prefactors as:

$$p(L) = [\mathcal{S}(2L, t = L/2) - \mathcal{S}(L, t = L/4)]/\log 2 \ . \tag{12}$$

From this series of results an estimate of c_{eff} or p is obtained by sequence extrapolation methods, such as by the Bulirsch-Stoer algorithm[33]. In the numerical calculation we used finite systems up to $L = 1024$ for the equilibrium entropy and up to $L = 512$ for the non-equilibrium entropy.

III. CHAIN WITH LOCALIZED DEFECTS

Having two symmetrically placed defects of strength Δ in the quantum Ising chain, as given by the Hamiltonian $H_0 + V_{ext}$ in Eqs.(4) and Eq.(6) we have calculated the entanglement entropy between two halves of the system for different lengths, L. The results are shown in Fig.1 as a function of $\log L$.

For large L the curves approach straight lines with different Δ-dependent slopes. We have calculated effective central charges by two point fits, see Eq.(11), and their extrapolated values are put in Fig. 2. These are continuous function of the strength of the defect and vary from 0 to 1/2 as Δ tuned from 0 to 1. The numerical data are consistent with the relation, $c_{eff}(\Delta) = c_{eff}(1/\Delta)$, which symmetry holds also for the local magnetization exponent in Eq.(8). For small Δ we have calculated $\mathcal{S}(L)$ perturbatively, the calculation is presented in Appendix B. We have obtained that in leading order of Δ^2, $\mathcal{S}(L)$ has a logarithmic L-dependence and the effective central charge is given by:

$$c_{eff}(\Delta) = 6\Delta^2 \left(\frac{1}{\pi^2}(1 - \ln \Delta^2) + b \right) + O(\Delta^4) \ . \tag{13}$$

Here $b = 0.062180(2)$ is a numerically calculated con-

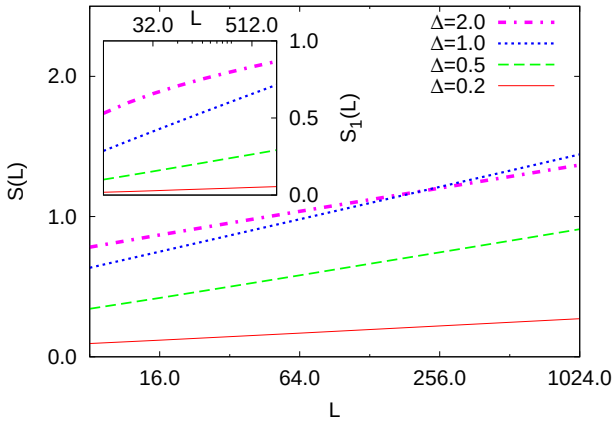

FIG. 1: (Color online) Entanglement entropy of the quantum Ising chain with different strength of the defect as a function of the logarithm of the length. Inset: the same for the single-copy entanglement.

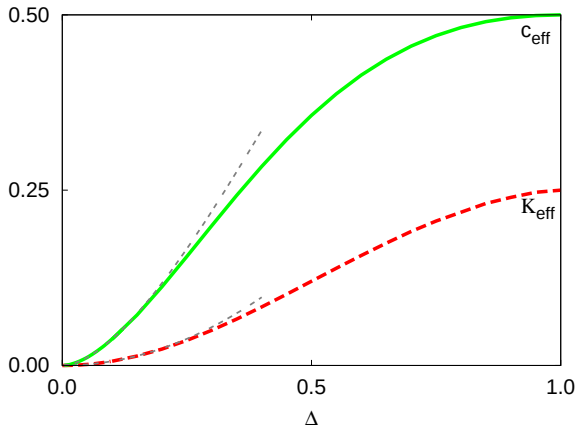

FIG. 2: (Color online) Effective central charge, $c_{eff}(\Delta)$ (full line - green), and the parameter, $\kappa_{eff}(\Delta)$ (broken line - red), of the single-copy entanglement of the quantum Ising chain as a function of the strength of the localized defect, Δ. For small Δ the leading behaviors obtained by perturbational calculation are indicated by dotted lines.

stant. The perturbative result in Eq.(13) is also shown in Fig.2 together with the numerical data. It is interesting to note that in Eq.(13) there is a logarithmic correction to the leading Δ^2 behavior.

We have also calculated the single-copy entanglement, $\mathcal{S}_1$, which is found to be in the form of Eq.(10), however with Δ dependent prefactors, $\kappa_{eff}(\Delta)$, the extrapolated values of which are plotted in Fig.2, too. In the range $0 < \Delta < 1$, $\kappa_{eff}(\Delta)$ is seen to vary between 0 and 1/4 and in the small Δ limit we have (see Appendix B):

$$\kappa_{eff}(\Delta) = \frac{6\Delta^2}{\pi^2} + O(\Delta^4) \, . \tag{14}$$

The ratio $\kappa_{eff}(\Delta)/c_{eff}(\Delta)$ varies between 0 and 1/2, thus the conformal result, $\kappa/c = 1/2$ is valid only in the homogeneous system.

Our results can be generalized if there is one defect in the system. For the closed chain (with $\Delta' = 1$) the effective central charge is changed to $(c_{eff}(\Delta) + 1/2)/2$, whereas for an open chain (with $\Delta' = 0$) the prefactor of the logarithm is just the half as for two defects.

A. Time evolution after the quench

Here we calculate the time evolution of the entropy by starting with two disconnected parts, i.e. with $\Delta = 0$ (and $\Delta' = 0$) for $t < 0$, and connecting them by one or two defects with $\Delta > 0$ for $t > 0$. In a finite chain of length L the entropy has a periodic time-dependence, the period of which is $L/2$, if the final chain is closed ($\Delta' = \Delta$ or $\Delta' = 1$.) and the period is L, if the final chain is open ($\Delta' = 0$.). This is illustrated in Fig.3 for a chain with $L = 128$ sites and with different type of defects.

If we perform the quench to the homogeneous chain, the numerical data are very well fitted by the formula:

$$\mathcal{S}_L^{cl}(t) = 2\frac{c}{3} \log \left| \frac{L}{2\pi} \sin \frac{2\pi t}{L} \right| + \text{cst} \, , \tag{15}$$

for a closed chain and

$$\mathcal{S}_L^{op}(t) = \frac{c}{3} \log \left| \frac{L}{\pi} \sin \frac{\pi t}{L} \right| + \text{cst} \, , \tag{16}$$

for an open chain with $c = 1/2$, which are also shown in Fig.3.

In the general case, when the closed chain for $t > 0$ contain one or two defects of strengths $0 < \Delta < 1$, the numerical results in Fig.3 are compatible with the scaling form (for closed chains):

$$\mathcal{S}_L^{cl}(t) = 2\frac{c_{eff}}{3} \log \left[L f^{cl}\left(\frac{t}{L}\right) \right] + \text{cst} \, , \tag{17}$$

where the scaling function, $f^{cl}(y) > 0$, is periodic with period 1/2 and for small argument it behaves as $f^{cl}(y) \sim y$. For an open chain with one defect the prefactor in

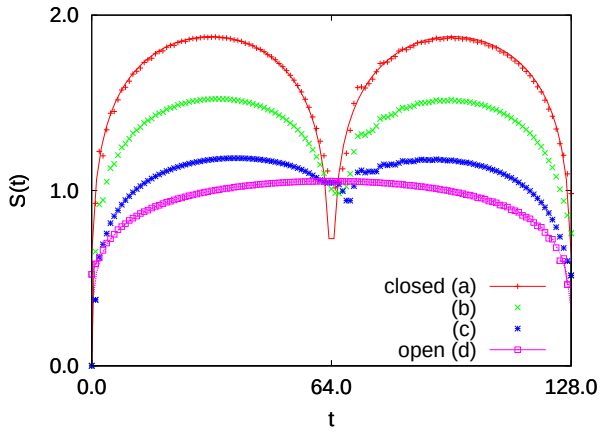

FIG. 3: (Color online) Time evolution of the entropy after a quench from two disconnected chains. The final system is closed and homogeneous (a) or contains one (b) or two (c) defects of strength $\Delta = 1/2$. The quench to a homogeneous open chain is given by (d). The analytical formulae for the homogeneous closed Eq.(15) and open Eq.(16) chains are also shown by full lines.

Eq.(17) is changed to its half and the scaling function, $f^{op}(y) > 0$, is periodic with period 1. Then for $t \ll L$ we expect the asymptotic behavior:

$$\mathcal{S}_L^{op}(t) \simeq \frac{c_{eff}}{3} \log t + \text{cst} \, , \tag{18}$$

which is a generalization of Eq.(3). This relation is

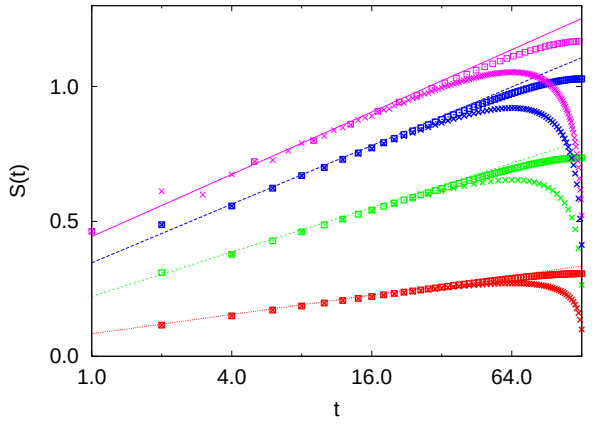

FIG. 4: (Color online) Time evolution of the entropy after a quench from two disconnected chains into an open chain with one defect having different strengths $\Delta = 1.$ (homogeneous), $\Delta = .75$, $\Delta = .5$ and $\Delta = .25$, from the top to the buttom. In the $\log t$ scale the initial part of the curves for $L = 128$ and $L = 256$ are close to the indicated straight lines having the slope $c_{eff}(\Delta)/3$, which is calculated from the scaling of the equilibrium entropy (see Fig.2).

checked in Fig.4 in which the time evolution of the entropy is shown as a function of $\log t$ for different values

of Δ. Indeed the starting part of the curves are well described by straight lines the slope of which is compatible with $c_{eff}(\Delta)/3$, as calculated from the equilibrium entropy and given in Fig.2.

We have repeated the calculation by considering another type of quench: for $t < 0$ the system contains a pair of defects of strength $0 < \Delta < 1$, which is changed to the homogeneous coupling, i.e. $\Delta = 1$ for $t > 0$. In this case the scaling form in Eq.(17) is still applicable, however with a different effective central charge, $c'_{eff}(\Delta)$, which is a decreasing function of Δ. We have checked that $c_{eff}(\Delta) + c'_{eff}(\Delta) = \tilde{c}(\Delta) > 1/2$, for example $\tilde{c}(.25) = 0.527(3)$, $\tilde{c}(.5) = 0.545(5)$ and $\tilde{c}(.75) = 0.520(5)$.

IV. CHAIN WITH EXTENDED DEFECTS

We have calculated the entanglement entropy between two halves of the quantum Ising chain which contains a pair of extended defect, as described by the Hamiltonian $H_0 + H_{ext}$ in Eqs.(4) and (9). For different lengths of the chain, L, the entropy is plotted in Fig.5 as a function of the strength of the defect, A.

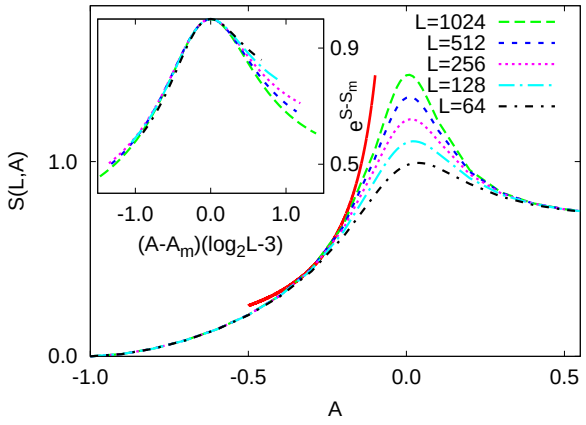

FIG. 5: (Color online) The entanglement entropy of the quantum Ising chain with two symmetrically placed extended defects as a function of the strength of the defect, A, for different finite systems. The conjectured asymptotic behavior in Eq.(20) is indicated by the full red curve. Inset: Scaling plot of the entanglement entropy around its maxima ($\exp(S-S_m)$) in terms of the combination $(A-A_m)(\log_2 L-3)$, see the text.

For a given L the entropy has a maximum close to $A = 0$, which corresponds to the critical pure system, whereas for large negative (positive) A the entropy approaches the limiting value 0 ($\log 2$), which is the same in the fully disordered (ordered) phase of the pure system. For intermediate values of $A \neq 0$ the entropy with increasing L seems to be saturated. This follows from the observation, that the effective central charges obtained through Eq.(11) approach zero even for a small value of $|A|$.

The finite-size dependence of the entropy can be explained if we take into account the critical scaling behavior at the interface, which is valid for large enough lengths, $L > \tilde{L}$. As described in Sec.II, for $A < 0$ the defect renormalizes to a cut, whereas for $A > 0$ it becomes ordered, which is in agreement with the behavior of the entropy in Fig.5. The microscopic length-scale, $\tilde{L}$, can be estimated in the $A < 0$ regime from the value of the renormalized connecting coupling: $J_0(L)|_{L=\tilde{L}} \sim \tilde{L}^{-|A|}$, which should be in the order of $O(1)$, say $e^{-\gamma}$, with $\gamma > 0$. From this we obtain for the microscopic length:

$$\tilde{L} \sim \exp\left(\frac{\gamma}{|A|}\right) . \qquad (19)$$

A similar expression can be derived in the regime $A > 0$, too. Note that $\tilde{L}$ has a very fast increase with decreasing $|A|$ and it is divergent in the homogeneous system. The microscopic length, $\tilde{L}$, sets in a length scale for the entanglement, too, and in the limit $\tilde{L} \ll L$ the entanglement entropy is obtained from Eq.(2) by replacing ξ with $\tilde{L}$, so that

$$\mathcal{S}(A) \simeq \frac{c}{3}\log\tilde{L} + \text{cst} \simeq \frac{c}{3}\frac{\gamma}{|A|} + \text{cst} . \qquad (20)$$

We have tried to fit the extrapolated numerical values of $\mathcal{S}(A)$ by this formula in Fig.5, which is found to be reasonable with $\gamma \simeq 0.87$.

We have also analyzed the finite-size scaling behavior of the entropy close to its maximum, which is located at $A_m = A_m(L)$ and has a value $\mathcal{S}_m = \mathcal{S}_m(L)$. In order to shift the maximum to the same position for all L we have considered the difference, $\Delta\mathcal{S}(L) \equiv \mathcal{S}(L) - \mathcal{S}_m$ as a function of $\Delta A \equiv A - A_m$. In terms of the scaling variable $\Delta A(\log L - 3)$ the curves for different L are scaled together, as illustrated in the inset of Fig.5. Here the scaling collapse is very good for $A < 0$, whereas for $A > 0$ the somewhat less perfect collapse is probably due to the presence of interface order in the system. Since $A_m(L) \to 0$ for large L the scaling combination used in the inset of Fig.5 is compatible with the microscopic length-scale defined in Eq.(19).

A. Time evolution after the quench

We have measured the time evolution of the entropy, if the system contains a pair of extended defects for $t < 0$, which is removed for $t > 0$ and we are left with the homogeneous closed chain. As shown in Fig.6 the entropy for $t \ll L$ has a logarithmic increase in time and the prefactor, $p(A)$, which seems to have the symmetry: $p(A) = p(-A)$ is increasing with $|A|$. We have calculated two-point fits for the prefactors, see in Eq.(12), the extrapolated values of which are plotted in the inset of Fig.6. The prefactor has its minimum around $A = 0$, which is close to $2c/3 = 1/3$, whereas for large $|A|$ we have approximately: $p(A) \approx A/2$. The

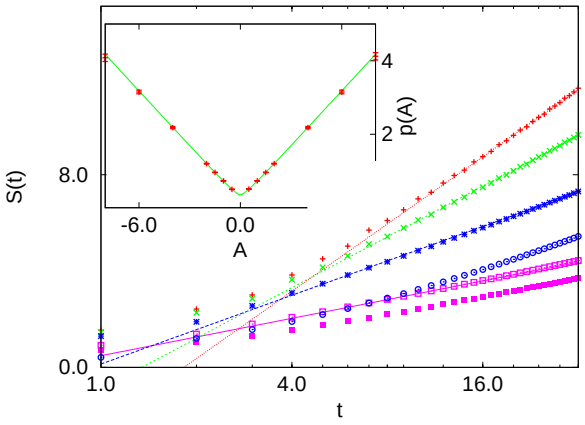

FIG. 6: (Color online) Time evolution of the entropy after removing a pair of extended defect of various strength, A, from the critical quantum Ising chain (for $t > 8$. from the top to the bottom A=-8.;-6.;-4.;4.;-2.;2.). In a $\log t$ plot the initial part of the curves are described by straight lines with A dependent slopes. The extrapolated values of the slopes as a function of A are given in the inset together with an interpolation curve, see the text.

measured points can be well interpolated by the curve: $p(A) = [1/9 + |A|/6 + A^2/4]^{1/2}$, which is also indicated in the inset of Fig.6.

To explain the observed behavior of the entropy we have to take into account two different effects of the extended defect. First, from local scaling consideration in Sec.II the defect renormalizes to a cut, thus - for small $|A|$ - the quench is made from two disconnected parts to a closed chain, and according to Eq.(15) the prefactor is $2c/3 = 1/3$ in agreement with the measured limiting values. The second effect of the extended defect is to produce an increase of the entropy through inhomogeneous quench, since the interaction in the chain at position x differs from the critical value by $J(x) - 1$. According to the argument in Ref.[5] pairs of quasiparticles are emitted at different points of the chain and they will contribute to the entanglement at later time, when reach the two parts of the system. The density of quasiparticles, $\alpha(x)$ depends on the distance from the critical point at the given position[34], and for a small perturbation it is given by[18] $\alpha \simeq |J(x) - 1|/2$. The increase of the entropy is obtained by integrating over the contributions:

$$\mathcal{S}(t) - \mathcal{S}(0) = \frac{1}{2}\int_{-t}^{t} \mathrm{d}x \alpha[J(x)] \,, \qquad (21)$$

which for the smooth inhomogeneity in Eq.(9) and for $t \ll L$ results in: $\mathcal{S}(t) - \mathcal{S}(0) \approx A/2 \log t$, in agreement with the numerical results.

V. DISCUSSION

In this paper we have considered the quantum Ising chain with critical couplings which is separated into two parts by localized or extended defects. In both cases the scaling behavior of the interface magnetization is non-universal (the scaling exponents depend on the strength of the defect) and we asked the question, how this fact is reflected in the entanglement properties of the system. For the localized defect both the equilibrium and the nonequilibrium entropy is found to be characterized by the same effective central charge, the value of which depends on the strength of the defect. In this case scaling of the equilibrium and the nonequilibrium entropy can be cast into the same form, see Eq.(17).

The situation is found completely different for the extended defect, in which case the equilibrium entropy is saturated, although the magnetization correlations (also at the interface) are long ranged and thus the corresponding correlation length is divergent. In this case the entanglement is related to another, finite microscopic length, as given in Eq.(19). This is due to the fact that the two parts of the system at the interface are asymptotically separated and the wave-function become localized. We can thus conclude that for an extended defect the correlation length and the entanglement length have different scaling properties. As far as the nonequilibrium entropy of this system is concerned it is shown to have a logarithmic t-dependence, the prefactor of which is the result of two effects: the asymptotic cut and the inhomogeneous quench.

Our results for the localized defect are related to similar studies for the XX-chain[21,22]. Since the entropy of the quantum Ising chain and that of the XX-chain are exactly related[35] the same is true for the central charges, too. For example from $c_{eff}(\Delta)$ in Fig.2 we obtain the effective central charge in the closed XX-chain with one interface defect of strength $t = \Delta$ as $c^{XX}_{eff}(t) = c_{eff}(\Delta) + 1/2$, as given in Fig.5 of Ref.[21]. Here we comment on the observation in Ref.[21] that the small Δ dependence of the effective central charge is given by: $c_{eff}(\Delta) \sim \Delta^{\delta}$, with an exponent, $\delta \approx 1.8$. According to our perturbative calculation in Eq.(13) the true exponent is $\delta = 2$, however with a multiplicative logarithmic correction term[36]. Similar behavior is expected to hold in higher dimensional gapless fermionic systems with weak links[37]. The result in Eq.(13) can be compared with a bosonization study of the continuum version of the XX-chain[22], in which the impurity (defect) contribution to the entanglement entropy is found to scale as:

$$\delta\mathcal{S} = \frac{1}{4} y^2 \epsilon^2 \ln\frac{L}{\epsilon}\left(1 - \ln\frac{L}{\epsilon}\right) \,, \qquad (22)$$

where y is the strength of the impurity potential and ϵ is a small-distance cutoff. The leading $\ln^2(L/\epsilon)$ term in Eq.(22) is not compatible with our lattice result.

As far as marginal extended defects are concerned our results for the nonequilibrium entropy are expected to

be generic for another critical quantum spin chains, too. From scaling theory it is known that an extended defect in the form, $(A/x)^\omega$, x being the distance from the center of the defect, is a marginal perturbation, provided $\omega = 1/\nu$, ν being the correlation length exponent[19]. Now estimating the nonequilibrium entropy we repeat the argument at the end of Sec.IV, where the density of quasiparticles is expected to scale with the value of the local gap[38]: $\alpha(x) \sim |J(x) - 1|^\nu \sim A/x$. Integrating the contributions in time, see Eq.(21), for large A leads to the behavior, $\mathcal{S}(t) - \mathcal{S}(0) \sim A \log t$, as for the quantum Ising chain.

This work has been supported by the Hungarian National Research Fund under grant No OTKA TO48721, K62588, K75324 and MO45596 and by a German-Hungarian exchange program (DFG-MTA). We are grateful to I. Peschel and H. Rieger for useful discussions.

APPENDIX A: TIME EVOLUTION OF THE ENTROPY FOR QUADRATIC FERMIONIC SYSTEMS

Let us consider a general Hamiltonian, $\mathcal{H}$, which is quadratic in terms of fermion creation, $c_k^\dagger$, and annihilation, c_k, operators and which is given for $t \geq 0$ as:

$$\mathcal{H} = \sum_{k,l=1}^{L} \left[c_k^\dagger A_{kl} c_l + \frac{1}{2} \left(c_k^\dagger B_{kl} c_l^\dagger + \text{h.c.} \right) \right] . \qquad \text{(A1)}$$

Here $A_{kl} \equiv (\mathbf{A})_{kl} = A_{lk}$ and $B_{kl} \equiv (\mathbf{B})_{kl} = -B_{lk}$ are real numbers and k, l are the sites of a lattice. In the initial state, i.e. for $t < 0$ the parameters of the Hamiltonian are different, say, $A_{kl}^{(0)}$ and $B_{kl}^{(0)}$ and the ground state of the initial Hamiltonian, $\mathcal{H}^{(0)}$, is denoted by $|\psi_0\rangle$. The system is divided into two parts: $\mathcal{A}$ consists of points $k = 1, 2, \ldots, \ell$ and $\mathcal{B}$ of the rest of the system.

For one dimensional spin models, such as the quantum Ising chain, the Pauli spin-operators, $\sigma_l^{x,y,z}$, are related to the fermionic operators as[29]:

$$\begin{aligned} \prod_{j<l} (-\sigma_j)^z \sigma_l^x &= c_l^\dagger + c_l \equiv \mathfrak{A}_l \equiv (-1)^{l-1} \check{a}_{2l-1} \\ \prod_{j<l} (-\sigma_j)^z \imath \sigma_l^y &= c_l^\dagger - c_l \equiv \mathfrak{B}_l \equiv (-1)^{l-1} \check{a}_{2l} . \end{aligned} \qquad \text{(A2)}$$

Here, in the last two equations, at a given site, l, we define two Clifford operators, $\mathfrak{A}_l$ and $\mathfrak{B}_l$, as well as two Majorana fermion operators, $\check{a}_{2l-1}$ and $\check{a}_{2l}$. The commutation relations for these new set of operators are:

$$\begin{aligned} \mathfrak{A}_l^2 = 1, \quad \mathfrak{B}_l^2 = -1, \quad \mathfrak{A}_l \mathfrak{B}_k = -\mathfrak{B}_k \mathfrak{A}_l, \\ \mathfrak{A}_l \mathfrak{A}_k = -\mathfrak{A}_k \mathfrak{A}_l, \quad \mathfrak{B}_l \mathfrak{B}_k = -\mathfrak{B}_k \mathfrak{B}_l, \quad l \neq k \end{aligned} \qquad \text{(A3)}$$

for the Clifford operators and

$$\check{a}_l^+ = \check{a}_l, \quad \{\check{a}_l, \check{a}_k\} = 2\delta_{l,k} \qquad \text{(A4)}$$

for the Majorana fermion operators.

The *first step* of the calculation is to diagonalize both , $\mathcal{H}^{(0)}$ and $\mathcal{H}$, which can be made by the same type of canonical transformation. For simplicity we work here with $\mathcal{H}$, for $\mathcal{H}^{(0)}$ the analogous results are denoted by a superscript $^{(0)}$. The new set of fermion operators are given by the combination:

$$\eta_k = \sum_l (g_{kl} c_l + h_{kl} c_l^\dagger) \qquad \text{(A5)}$$

where g_{kl} and h_{kl} are real numbers and the Hamiltonian assumes the diagonal form:

$$\mathcal{H} = \sum_{k=1}^{L} \Lambda_k \eta_k^\dagger \eta_k + \text{const.} , \qquad \text{(A6)}$$

Here the energy of the free-fermionic modes, Λ_k, are given by the solution of the eigenvalue equations:

$$\begin{aligned} (\mathbf{A} - \mathbf{B})(\mathbf{A} + \mathbf{B}) \mathbf{\Phi}_k &= \Lambda_k^2 \mathbf{\Phi}_k \\ (\mathbf{A} + \mathbf{B})(\mathbf{A} - \mathbf{B}) \mathbf{\Psi}_k &= \Lambda_k^2 \mathbf{\Psi}_k . \end{aligned} \qquad \text{(A7)}$$

and the components of the eigenvectors are:

$$\begin{aligned} \Phi_k(i) &= g_{ki} + h_{ki} \\ \Psi_k(i) &= g_{ki} - h_{ki} . \end{aligned} \qquad \text{(A8)}$$

In the *second step* we consider the subsystem $\mathcal{A}$ and calculate its reduced density matrix, ρ_A, which can be reconstructed from the time-dependent reduced correlation matrix of the Majorana operators:

$$\langle \psi_0 | \check{a}_m(t) \check{a}_n(t) | \psi_0 \rangle = \delta_{m,n} + \imath (\Gamma_\ell^A)_{mn} , \qquad \text{(A9)}$$

$m, n = 1, 2, \ldots, 2\ell$. Here $(\Gamma_\ell^A)_{mn}$ is a skew-symmetric (or antisymmetric) matrix which is transformed by an orthogonal transformation, Q, into a block-diagonal form:

$$Q \Gamma_\ell^A Q^T = \begin{bmatrix} 0 & \nu_1 & 0 & 0 & \ldots & & \\ -\nu_1 & 0 & 0 & 0 & \ldots & & \\ 0 & 0 & 0 & \nu_2 & \ldots & & \\ 0 & 0 & -\nu_2 & 0 & \ldots & & \\ & & & & \ddots & & \\ & & & & \ldots 0 & \nu_r & \\ & & & & \cdots -\nu_r & 0 & \\ & & & & & & \ddots \end{bmatrix} \qquad \text{(A10)}$$

thus the eigenvalues of Γ_ℓ^A are $\pm \imath \nu_r$, $r = 1, 2, \ldots, \ell$. In this representation the reduced density matrix is the direct product of ℓ uncorrelated modes: $\rho_\ell = \bigotimes_{r=1}^{\ell} \rho_r$, where ρ_r has eigenvalues $(1 \pm \nu_r)/2$. The entanglement entropy is then given by the sum of binary entropies:

$$S_L(\ell) = -\sum_{r=1}^{\ell} \left(\frac{1+\nu_r}{2} \log_2 \frac{1+\nu_r}{2} + \frac{1-\nu_r}{2} \log_2 \frac{1-\nu_r}{2} \right) . \qquad \text{(A11)}$$

In the *third step* we calculate the time-dependent correlation matrix and work in terms of the Clifford-operators the time evolution of which are given by[32]:

$$\mathfrak{A}_l(t) = \sum_k \left[\langle A_l A_k\rangle_t \mathfrak{A}_k + \langle A_l B_k\rangle_t \mathfrak{B}_k\right]$$
$$\mathfrak{B}_l(t) = \sum_k \left[\langle B_l A_k\rangle_t \mathfrak{A}_k + \langle B_l B_k\rangle_t \mathfrak{B}_k\right] \qquad \text{(A12)}$$

Here the time-dependent contractions are:

$$\begin{aligned}
\langle A_l A_k\rangle_t &= \sum_q \cos(\Lambda_q t)\Phi_q(l)\Phi_q(k)\ ,\\
\langle A_l B_k\rangle_t &= \langle B_k A_l\rangle_t = i\sum_q \sin(\Lambda_q t)\Phi_q(l)\Psi_q(k)\ ,\\
\langle B_l B_k\rangle_t &= \sum_q \cos(\Lambda_q t)\Psi_q(l)\Psi_q(k)\ . \qquad \text{(A13)}
\end{aligned}$$

Note, that in Eq.(A13) the free-fermionic quantities are related to the Hamiltonian $\mathcal{H}$, which governs the time evolution in the system for $t > 0$. The matrix-elements of the time-dependent Clifford operators, such as $\langle\psi_0|\mathfrak{A}_l(t)\mathfrak{A}_k(t)|\psi_0\rangle$, involve the following ground-state expectation values:

$$\begin{aligned}
&\langle\psi_0|\mathfrak{A}_{k_1}\mathfrak{A}_{k_2}|\psi_0\rangle = \delta_{k_1,k_2},\ \langle\psi_0|\mathfrak{B}_{k_1}\mathfrak{B}_{k_2}|\psi_0\rangle = -\delta_{k_1,k_2}\\
&\langle\psi_0|\mathfrak{A}_{k_1}\mathfrak{B}_{k_2}|\psi_0\rangle = -G^{(0)}_{k_2k_1},\ \langle\psi_0|\mathfrak{B}_{k_1}\mathfrak{A}_{k_2}|\psi_0\rangle = G^{(0)}_{k_1k_2} \qquad \text{(A14)}
\end{aligned}$$

Here the first equations follow from the commutation rules in Eq.(A3), whereas the static correlation matrix $G^{(0)}_{k_1k_2}$ is given by:

$$G^{(0)}_{k_1k_2} = -\sum_q \Psi^{(0)}_q(k_1)\Phi^{(0)}_q(k_2)\ , \qquad \text{(A15)}$$

which is calculated with the initial Hamiltonian, $\mathcal{H}^{(0)}$. Now one can go on and calculate the time-dependent correlation matrix of the Clifford operators, which is then transformed by Eq(A2) for Majorana operators so that finally one obtains the matrix-elements of Γ^A in Eq.(A9) as:

$$\begin{aligned}
\Gamma^A_{2l-1,2m-1} &= -\imath\left[\sum_{k_1,k_2} G^{(0)}_{k_1k_2}\langle A_l B_{k_1}\rangle_t\langle A_m A_{k_2}\rangle_t - \sum_{k_1,k_2} G^{(0)}_{k_2k_1}\langle A_l A_{k_1}\rangle_t\langle A_m B_{k_2}\rangle_t\right](-1)^{l+m}\\
\Gamma^A_{2l-1,2m} &= \left[\sum_{k_1,k_2} G^{(0)}_{k_2k_1}\langle A_l A_{k_1}\rangle_t\langle B_m B_{k_2}\rangle_t - \sum_{k_1,k_2} G^{(0)}_{k_1k_2}\langle A_l B_{k_1}\rangle_t\langle B_m A_{k_2}\rangle_t\right](-1)^{l+m}\\
\Gamma^A_{2l,2m-1} &= -\left[\sum_{k_1,k_2} G^{(0)}_{k_2k_1}\langle A_m A_{k_1}\rangle_t\langle B_l B_{k_2}\rangle_t - \sum_{k_1,k_2} G^{(0)}_{k_1k_2}\langle A_m B_{k_1}\rangle_t\langle B_l A_{k_2}\rangle_t\right](-1)^{l+m}\\
\Gamma^A_{2l,2m} &= -\imath\left[\sum_{k_1,k_2} G^{(0)}_{k_2k_1}\langle B_l A_{k_1}\rangle_t\langle B_m B_{k_2}\rangle_t - \sum_{k_1,k_2} G^{(0)}_{k_1k_2}\langle B_l B_{k_1}\rangle_t\langle B_m A_{k_2}\rangle_t\right](-1)^{l+m} \qquad \text{(A16)}
\end{aligned}$$

APPENDIX B: PERTURBATIVE CALCULATION OF THE ENTROPY FOR LOCALIZED DEFECTS

Here we consider the homogeneous quantum Ising chain with one single defect coupling of strength, Δ, between spins at ℓ and $\ell+1$, but the two ends of the chain at 1 and L are free. The unperturbed system (with $\Delta = 0$) consists of two separated chains: $\mathcal{A}$ with sites $i = 1, 2, \ldots \ell$ and $\mathcal{B}$ with sites $i = \ell+1, \ell+2, \ldots L$, and the length of $\mathcal{B}$ is denoted by $\ell' = L - \ell$. The reduced density matrix of $\mathcal{A}$, denoted by ρ_ℓ, is calculated perturbatively in Ref.[35]. The matrix-elements in leading order, i.e. up to $O(\Delta^2)$ are given by:

$$\langle\varphi^{\mathcal{A}}_i|\rho_\ell|\varphi^{\mathcal{A}}_j\rangle = \rho_\ell(i,j) = \mathcal{Z}\sum_k^{\mathcal{B}} c(i,k)c^*(j,k)\ , \qquad \text{(B1)}$$

with $c(0,0) = 1$ and

$$c(i,k) = \frac{\Delta}{E^{\mathcal{A}}_i + E^{\mathcal{B}}_k}\langle\varphi^{\mathcal{A}}_i|\sigma^x_\ell|\varphi^{\mathcal{A}}_0\rangle\langle\varphi^{\mathcal{B}}_k|\sigma^x_{\ell+1}|\varphi^{\mathcal{B}}_0\rangle\ . \qquad \text{(B2)}$$

Here $|\varphi^{\mathcal{A}}_i\rangle$ ($|\varphi^{\mathcal{B}}_k\rangle$) is the i-the (k-th) eigenstate of the unperturbed system $\mathcal{A}$ ($\mathcal{B}$) with excitation energy: $E^{\mathcal{A}}_i$ ($E^{\mathcal{B}}_k$) and $\mathcal{Z}$ is a normalization constant, so that $\sum_i^{\mathcal{A}}\rho_\ell(i,i) = 1$. In Eq.(B2) the matrix-elements of the surface magnetization operators σ^x_ℓ of system $\mathcal{A}$ and $\sigma^x_{\ell+1}$ of system $\mathcal{B}$ are non-zero, if the excited states, $|\varphi^{\mathcal{A}}_i\rangle$ and $|\varphi^{\mathcal{B}}_k\rangle$ in the fermionic representation contain just one fermion. Then using the notation of App.A the non-vanishing matrix-elements are given by: $\langle\varphi^{\mathcal{A}}_i|\sigma^x_\ell|\varphi^{\mathcal{A}}_0\rangle = \Psi^{\mathcal{A}}_i(\ell)$, $i = 1, 2, \ldots \ell$ with $E^{\mathcal{A}}_i = \Lambda^{\mathcal{A}}_i$ and $\langle\varphi^{\mathcal{B}}_k|\sigma^x_{\ell+1}|\varphi^{\mathcal{B}}_0\rangle = \Psi^{\mathcal{B}}_k(1)$, $k = 1, 2, \ldots \ell'$ with $E^{\mathcal{B}}_k = \Lambda^{\mathcal{B}}_k$. Using the exact solution of

the open quantum Ising chain with homogeneous critical couplings of length ℓ (see Eqs.(A.5) and (A.6) of Ref.[16]) we obtain in leading order:

$$\rho_\ell(i,j) = \mathcal{Z}\Delta^2 \frac{\cos\alpha_i \cos\alpha_j}{(2\ell+1)(2\ell'+1)} \times \sum_{k=1}^{\ell'} \frac{\cos^2\beta_k}{(\sin\alpha_i+\sin\beta_k)(\sin\alpha_j+\sin\beta_k)} \quad \text{(B3)}$$

$i,j = 1,2,\ldots,\ell$, with $\alpha_i = \frac{\pi}{2}\frac{2i-1}{2\ell+1}$ and $\beta_k = \frac{\pi}{2}\frac{2k-1}{2\ell'+1}$. In the following we analyse the consequences of this expression in the limits: $\ell \gg 1$ and $\ell'/\ell \gg 1$.

The leading eigenvalue of the reduced density matrix is:

$$w_1 = \mathcal{Z} = 1 - \Delta^2 \left(a_1 + a\log\ell\right) , \quad \text{(B4)}$$

where the prefactor of the logarithm is $a = \pi^{-2}$, and a_1 is a constant of $O(1)$. From Eq.(B4) we obtain for the single-copy entanglement:

$$\mathcal{S}_1 = \Delta^2 \left(\frac{1}{\pi^2}\log\ell + \text{cst.}\right) \quad \text{(B5)}$$

which is proportional to $\log\ell$. For *two* symmetrically placed defects, as studied numerically in Sec.III the prefactor is $2\Delta^2/\pi^2$, from which we obtain the value of $\kappa_{eff}(\Delta)$ as given in Eq.(14).

To obtain the entanglement entropy in leading order one should calculate the other $i = 2,3,\ldots\ell+1$ eigenvalues of the reduced density matrix, which are expressed as: $w_i = \Delta^2\epsilon_i$, so that the entropy is given by:

$$\mathcal{S}(\Delta) = -w_1\log w_1 - \Delta^2\sum_{i=2}^{\ell+1}\epsilon_i(\log\epsilon_i + \log\Delta^2) + O(\Delta^4) . \quad \text{(B6)}$$

Here the correction term is evaluated numerically and we have obtained $\sum_{i=2}^{\ell+1}\epsilon_i\log\epsilon_i = b_1 + b\log\ell$ and the prefactor of the logarithm is $b = 0.062180(2)$. Putting this and w_1 from Eq.(B4) into Eq.(B6) we obtain that the entanglement entropy scales as $\log\ell$ for large ℓ, and the effective central charge (calculated for *two* symmetrically placed defects) is given in Eq.(13).

[1] L. Amico, R. Fazio, A. Osterloh and V. Vedral, *Rev. Mod. Phys.* **80** 517 (2008).
[2] C. Holzhey, F. Larsen, and F. Wilczek, Nucl. Phys. B **424**, 443 (1994).
[3] G. Vidal, J. I. Latorre, E. Rico and A. Kitaev, Phys. Rev. Lett. **90**, 227902 (2003); J. I. Latorre, E. Rico and G. Vidal, *Quantum Inf. Comput.* **4** 48 (2004).
[4] P. Calabrese and J. L. Cardy, *J. Stat. Mech.* P06002 (2004).
[5] P. Calabrese and J. L. Cardy, *J. Stat. Mech.* P04010 (2005).
[6] V. Eisler and I. Peschel, *J. Stat. Mech.* P06005 (2007).
[7] P. Calabrese and J. L. Cardy, *J. Stat. Mech.* P10004 (2007).
[8] V. Eisler, D. Karevski, T. Platini and I. Peschel, *J. Stat. Mech.* P01023 (2008).
[9] G. Refael and J. E. Moore, *Phys. Rev. Lett.* **93** 260602 (2004).
[10] N. Laflorencie, *Phys. Rev. B* **72** 140408 (R) (2005).
[11] G. De Chiara, S. Montangero, P. Calabrese and R. Fazio, J. Stat. Mech. P03001 (2006).
[12] R. Santachiara, J. Stat. Mech. L06002 (2006).
[13] G. Refael and J. E. Moore, Phys. Rev. B **76** 024419 (2007).
[14] N. E. Bonesteel and K. Yang, Phys. Rev. Lett. **99** 140405 (2007).
[15] F. Iglói, Y.-C. Lin, H. Rieger and C. Monthus, Phys. Rev. B **76**, 064421 (2007).
[16] F. Iglói and Y-Ch Lin, *J. Stat. Mech.* P06004 (2008).
[17] F. Iglói, R. Juhász Z. Zimborás, Europhys. Lett.**79**, 37001 (2007).
[18] V. Eisler, F. Iglói and I. Peschel, J. Stat. Mech. P02011 (2009).
[19] F. Iglói, I. Peschel, and L. Turban, Advances in Physics **42**, 683 (1993).
[20] J. Zhao, I. Peschel and X. Wang, *Phys. Rev. B* **73** 024417 (2006).
[21] I. Peschel, *J. Phys. A: Math. Gen.* **38** 4327 (2005).
[22] G. C. Levine, *Phys. Rev. Lett.* **93** 266402 (2004).
[23] S. Eggert and I. Affleck, Phys. Rev. B **46**, 10866 (1992).
[24] H. J. Hilhorst and J. M. J. van Leeuwen, Phys. Rev. Lett. **47**, 1188 (1981).
[25] F. Iglói, B. Berche, and L. Turban, Phys. Rev. Lett. **65**, 1773 (1990).
[26] P. Pfeuty, Phys. Lett. **72A**, 245 (1979).
[27] R. Z. Bariev, Zh. Eksp. Teor. Fiz. **77** 1217 (Soviet Phys. JETP, **50**, 613 (1979)).
[28] B. M. McCoy and J. H. H. Perk, Phys. Rev. Lett. **44**, 840 (1980).
[29] E. Lieb, T. Schultz and D. Mattis, Annals of Phys. **16**, 407 (1961).
[30] I. Peschel, 2003 *J. Phys. A: Math. Gen.* **36** L205 (2003).
[31] I. Peschel and J. Zhao, J. Stat. Mech. P11002 (2005).
[32] F. Iglói and H. Rieger, Phys. Rev. Lett. **85**, 3233 (2000).
[33] R. Bulirsch and J. Stoer, Numer. Math. 6, 413 (1964).
[34] M. Fagotti and P. Calabrese, *Phys. Rev. A* **78** 010306(R) (2008).
[35] F. Iglói and R. Juhász, Europhys. Lett. **81**, 57003 (2008).
[36] We note that a similar correction term to the effective central charge in $c = 1$ conformal field theory with permeable interfaces has been derived recently, K. Sakai, and Y. Satoh, preprint arXiv:0809.4548.
[37] G. C. Levine and D. J. Miller, *Phys. Rev. B* **77** 205119 (2008).
[38] S. Sotiriadis and J. L. Cardy, J. Stat. Mech. P11003 (2008).